A Coherent Amplify-and-Forward Relaying Demonstrator Without Global Phase Reference

Stefan Berger, *Student Member, IEEE,* Armin Wittneben, *Member, IEEE*

I. Abstract

In this work we present a demonstrator for coherent linear amplify-and-forward (AF) relaying. Two source/destination pairs communicate with the help of three half-duplex relays in a two-hop manner. We implemented a coherent gain allocation scheme that suppresses inter-user interference at each destination and does not require a global phase reference at the relays. In order to assess the performance of the scheme, we calculated the signal-to-interference ratio (SIR) at both destination nodes. Inter-user interference arises when the local oscillator phases of the relays change independently during one transmission cycle, e.g. due to phase noise. Consequently, the shorter the time between reception and retransmission at the relays, the more accurate the interference suppression. Measurement results show that our demonstrator is able to suppress inter-user interference at both destinations reasonably well.

***Index Terms*—Demonstrator, multiuser relaying, distributed beamforming, coherent cooperative relaying**

II. Introduction

In recent years a lot of research has been done in the field of cooperative wireless communication, where a number of autonomous nodes cooperates in order to increase the link reliability and/or the data rate. The notion of (user) cooperative diversity was introduced in [1], [2], where spatial diversity is achieved by multiple antennas belonging to different users. In [3] capacity scaling laws in MIMO relay networks have been investigated and it was shown that asymptotically in the number of relays, full spatial multiplaxing gain can be achieved even when there is no channel knowledge at the relays.

In our work, we consider a system with finite number of half-duplex amplify-and-forward (AF) relays and multiple source/destination pairs. In the field of AF relaying, we generally distinguish between *coherent* and *noncoherent forwarding*. For coherent forwarding the signal processing at the relays takes the signal phase into account, whereas for noncoherent forwarding phase information is disregarded. Consequently, noncoherent forwarding schemes cannot achieve a distributed array gain. So far people assumed that coherent forwarding requires a global phase reference at the relays. Papers addressing the issue of synchronizing the local oscillator (LO) phases of distributed nodes are, e.g., [4], [5], and [6]. However, in a real world distributed network phase synchronization is difficult to achieve. In [7] we show that in some cases the relays do not require a global carrier phase reference in order to coherently forward the signal. We will give an intuition on the reasoning in **Section III** of this work. Two requirements allow for coherent relaying even when the relay phases are unknown and random:

1) The LO phase offsets at the relay terminals stay constant for at least one transmission cycle (consisting of reception and retransmission), and
2) all antennas at a relay have the same LO phase reference.

S. Berger and A. Wittneben are with ETH Zurich, Switzerland (e-mail: berger@nari.ee.ethz.ch, wittneben@nari.ee.ethz.ch)

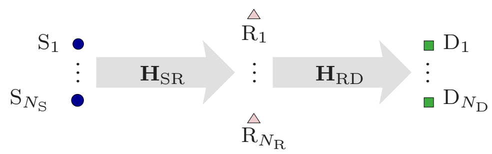

Fig. 1. Two-hop system configuration with half-duplex relays

The first requirement is related to phase noise (see e.g. [8]). The phase jitter at the LOs has to be small during the time of at least one transmission cycle. The second requirement is probably met in most real-world relaying scenarios.

In this work we present a demonstrator for coherent linear AF relaying. The system model is introduced in **Section III**, where our focus lies on the impact of phase noise and carrier frequency offset at the terminals to the system. In **Section IV** we describe the estimation of first-hop and second-hop channels. **Section V** treats the demonstrator itself. We introduce the RACooN Lab (a measurement equipment at our institute), as well as the system setup consisting of 2 source/destination pairs and 3 relays. Furthermore, we discuss the phase noise characteristic of the nodes and give details about the implemented two-hop transmission cycle. A measurement campaign was conducted using a gain allocation scheme that suppresses inter-user interference at both destinations [9] (multiuser zero-forcing relaying). Using the signal-to-interference ratio (SIR) at both destination nodes as figure of merit, we present our results in **Section VI**.

Notation: We use bold uppercase and lowercase letters to denote matrices and vectors, respectively. $\mathbf{X}[i,j]$ indicates the element in row i, column j of the matrix $\mathbf{X}$. The operator $(\cdot)^\mathrm{H}$ is the hermitian transpose and $\mathbf{I}_N$ the identity matrix of size $N \times N$. $\mathrm{diag}\,(\mathbf{x})$ writes the elements of the vector $\mathbf{x}$ into a diagonal matrix. Finally, a vector whose entries are taken from a circular symmetric complex normal distribution with mean vector μ and covariance matrix $\mathbf{\Sigma}$ is denoted by $\mathbf{x} \sim \mathcal{CN}\,(\mu, \mathbf{\Sigma})$.

III. System Model

We consider a distributed wireless network where N_S sources and N_D destinations communicate with the help of N_R linear amplify-and-forward relay nodes. All nodes in the network employ a single antenna only. The communication includes two channel uses: one for the *first-hop* transmission from the sources S_k, $k \in \{1,\ldots,N_\mathrm{S}\}$ to all relays R_l, $l \in \{1,\ldots,N_\mathrm{R}\}$ and one for the *second-hop* transmission from the relays to the destinations D_m, $m \in \{1,\ldots,N_\mathrm{D}\}$ (see **Fig. 1**). For the sake of simplicity we do not take the direct link into account. The relays amplify the signals they receive from the sources by multiplication with complex gain factors before retransmitting them. All channel coefficients are assumed to be independent, frequency flat, complex Gaussian random variables with circular symmetric probability density function (Rayleigh fading):

$$\mathbf{H}_{\mathrm{SR}}[l,k] \sim \mathcal{CN}\left(0,\sigma_h^2\right)$$
$$\mathbf{H}_{\mathrm{RD}}[m,l] \sim \mathcal{CN}\left(0,\sigma_h^2\right) \quad (1)$$

for all $k \in \{1,\dots,N_{\mathrm{S}}\}$, $l \in \{1,\dots,N_{\mathrm{R}}\}$, and $m \in \{1,\dots,N_{\mathrm{D}}\}$. In order to introduce the system model, the channels are assumed to be constant during at least one transmission cycle while different channel realizations are temporally uncorrelated (block fading).

Every node employs a free running LO. Let $\phi_{\mathrm{x}}(t)$ denote the phase offset of the LO of terminal x with respect to a global phase reference at time instant t. We can write

$$\phi_{\mathrm{x}}(t) = 2\pi f_{\mathrm{x}} t + \varphi_{\mathrm{x}}(t) \quad (2)$$

where f_{x} is the carrier frequency and $\varphi_{\mathrm{x}}(t)$ an unknown and random phase offset due to phase noise. We make the following assumptions regarding phase noise and carrier frequency:

- **Phase noise**: The phase offset $\varphi_{\mathrm{x}}(t)$ is a Wiener-Lévy process (Wiener phase noise). This assumption is widely used in OFDM literature to model phase noise and analyze its effect (e.g [10]). It describes the phase variations of a free running oscillator that is disturbed by white noise [8]. In this case the phase at time $t = t_0 + \Delta t$ is a Gaussian random variable with variance $\Delta t \cdot \sigma_{\mathrm{pn}}^2$ and mean $\varphi_{\mathrm{x}}(t_0)$. We write
$$\varphi_{\mathrm{x}}(t) = \varphi_{\mathrm{x}}(t_0) + \psi_{\mathrm{x}}, \quad (3)$$
where $\psi_{\mathrm{x}} \sim \mathcal{N}\left(0, \Delta t \cdot \sigma_{\mathrm{pn}}^2\right)$.
- **Carrier frequency**: Although the individual carrier frequencies might be slightly different for each terminal, they can be assumed as stable compared to phase noise and channel variations. Thus the nodes can synchronize and we assume $f_{\mathrm{x}} = f_{\mathrm{c}}$ for all nodes x.

We rewrite (2) according to our model as

$$\phi_{\mathrm{x}}(t) = 2\pi f_{\mathrm{c}} t + \varphi_{\mathrm{x}}(t_0) + \psi_{\mathrm{x}}. \quad (4)$$

Assume that node i wants to transmit the complex baseband symbol s over the scalar channel $h_{ji} \sim \mathcal{CN}\left(0,\sigma_{\mathrm{h}}^2\right)$ to node j. Neglecting any noise, node j receives

$$d = h_{ji} \cdot e^{j(2\pi f_{\mathrm{c}} t + \varphi_{\mathrm{i}}(t_0) + \psi_{\mathrm{i}})} e^{j\left(-2\pi f_{\mathrm{c}} t - \varphi_{\mathrm{j}}(t_0) - \psi_{\mathrm{j}}\right)} \cdot s =$$
$$= h_{ji} \cdot e^{j\left(\varphi_{\mathrm{i}}(t_0) - \varphi_{\mathrm{j}}(t_0)\right)} e^{j\left(\psi_{\mathrm{i}} - \psi_{\mathrm{j}}\right)} \cdot s \quad (5)$$

As h_{ji} is a circular symmetric random variable a constant phase rotation by $\varphi_{\mathrm{i}}(t_0) - \varphi_{\mathrm{j}}(t_0)$ does not change its statistics. We can thus write

$$d = h'_{ji} \cdot e^{j\left(\psi_{\mathrm{i}} - \psi_{\mathrm{j}}\right)} \cdot s, \quad (6)$$

where h'_{ji} has the same statistics as h_{ji}. In an ordinary single-hop link, the phase uncertainty due to the unknown LO phases can be compensated using a phase-locked-loop (PLL). Now we extend the considerations to the case where we have multiple sources, relays, and destination nodes (see **Fig. 1**). Dropping explicit time dependance, we write $\varphi_x := \varphi_x(t_0)$ for the LO phase offset of terminal x at a certain point in time t_0. The diagonal matrices

$$\mathbf{\Phi}_{\mathrm{X}} = \mathrm{diag}\left(e^{j\varphi_{\mathrm{X}_1}}, \dots, e^{j\varphi_{\mathrm{X}_{N_\mathrm{X}}}}\right), \ \mathrm{X} \in \{\mathrm{S}, \mathrm{R}, \mathrm{D}\} \quad (7)$$

then comprise the unknown and random phases of all sources, relays, and destinations, respectively, at t_0. In our model Wiener phase noise makes the LO phases change randomly between any two time instances (see (3)). These changes are introduced to the system in form of the matrices

$$\mathbf{\Psi}_{\mathrm{X}} = \mathrm{diag}\left(e^{j\psi_{\mathrm{X}_1}}, \dots, e^{j\psi_{\mathrm{X}_{N_\mathrm{X}}}}\right). \quad (8)$$

The received signal at the relays is

$$\mathbf{r} = \mathbf{\Phi}_{\mathrm{R}}^{\mathrm{H}} \mathbf{H}_{\mathrm{SR}} \mathbf{\Phi}_{\mathrm{S}} \mathbf{s} + \mathbf{n}_{\mathrm{R}}, \quad (9)$$

where the transmit symbols of all sources are stacked in the vector $\mathbf{s}$ and $\mathbf{n}_{\mathrm{r}}$ comprises additive white Gaussian noise (AWGN) at the relays. We assume that the transmit power of all sources is equal and the transmit symbols are mutually independent, i.e. $\mathrm{E}\left[\mathbf{s}\mathbf{s}^{\mathrm{H}}\right] = \sigma_{\mathrm{s}}^2 \mathbf{I}_{N_{\mathrm{S}}}$. With (8) the received signal at the destinations can be written as

$$\mathbf{d} = \mathbf{\Phi}_{\mathrm{D}}^{\mathrm{H}} \mathbf{H}_{\mathrm{RD}} \mathbf{\Phi}_{\mathrm{R}} \mathbf{\Psi}_{\mathrm{R}} \mathbf{G} \mathbf{r} + \mathbf{n}_{\mathrm{D}}, \quad (10)$$

where $\mathbf{G}$ is the diagonal *gain matrix* used at the relays and $\mathbf{n}_{\mathrm{D}}$ the vector of AWGN at the destinations. The noise covariance matrices are given by $\mathrm{E}\left[\mathbf{n}_{\mathrm{R}}\mathbf{n}_{\mathrm{R}}^{\mathrm{H}}\right] = \mathrm{E}\left[\mathbf{n}_{\mathrm{D}}\mathbf{n}_{\mathrm{D}}^{\mathrm{H}}\right] = \sigma_{\mathrm{n}}^2 \mathbf{I}_{N_{\mathrm{R}}}$. When the relays' LO phases stay constant for a whole transmission cycle, i.e. $\mathbf{\Psi}_{\mathrm{R}} = \mathbf{I}_{N_{\mathrm{R}}}$, we have $\mathbf{\Phi}_{\mathrm{R}} \mathbf{\Psi}_{\mathrm{R}} \mathbf{G} \mathbf{\Phi}_{\mathrm{R}}^{\mathrm{H}} = \mathbf{G}$ and thus

$$\mathbf{d} = \mathbf{\Phi}_{\mathrm{D}}^{\mathrm{H}} \mathbf{H}_{\mathrm{RD}} \mathbf{G} \mathbf{H}_{\mathrm{SR}} \mathbf{\Phi}_{\mathrm{S}} \mathbf{s} + \mathbf{\Phi}_{\mathrm{D}}^{\mathrm{H}} \mathbf{H}_{\mathrm{RD}} \mathbf{\Phi}_{\mathrm{R}} \mathbf{G} \mathbf{n}_{\mathrm{R}} + \mathbf{n}_{\mathrm{D}} =$$
$$= \mathbf{H}_{\mathrm{SRD}} \mathbf{s} + \mathbf{n}. \quad (11)$$

In this case, the relays' LO phase offsets do not have an impact on the received signal at the destinations. We defined the *equivalent channel matrix*

$$\mathbf{H}_{\mathrm{SRD}} = \mathbf{\Phi}_{\mathrm{D}}^{\mathrm{H}} \mathbf{H}_{\mathrm{RD}} \mathbf{G} \mathbf{H}_{\mathrm{SR}} \mathbf{\Phi}_{\mathrm{S}} \quad (12)$$

and the *equivalent noise vector*

$$\mathbf{n} = \mathbf{\Phi}_{\mathrm{D}}^{\mathrm{H}} \mathbf{H}_{\mathrm{RD}} \mathbf{\Phi}_{\mathrm{R}} \mathbf{G} \mathbf{n}_{\mathrm{R}} + \mathbf{n}_{\mathrm{D}}. \quad (13)$$

Under assumption 2) in section II, $\mathbf{\Phi}_{\mathrm{R}}$ does not influence the statistics of $\mathbf{n}$.

IV. Channel Estimation

For any coherent forwarding scheme, the relays require channel knowledge in order to calculate the gain matrix $\mathbf{G}$. In this section we shortly describe how the channel estimation is done in our system. We assume that the nodes are frequency but not phase synchronous. This is a sensible assumption as the frequency offsets will be quite stable and can be compensated using well-known techniques.

In order to estimate the *first-hop channel coefficients*, all source nodes transmit orthogonal training sequences to all relays. Knowing these sequences, each relay can estimate its local first-hop channel coefficients. Assuming a noiseless estimation, relay l can compute

$$\widehat{h}_{\mathrm{S}_k\mathrm{R}_l} = h_{\mathrm{S}_k\mathrm{R}_l} e^{j\left(\varphi_{\mathrm{S}_k} - \varphi_{\mathrm{R}_l}\right)}, \ \forall\, k = \{1, \dots, N_{\mathrm{S}}\}. \quad (14)$$

The matrix of estimated first-hop channel coefficients can thus be written as

$$\widehat{\mathbf{H}}_{\mathrm{SR}} = \mathbf{\Phi}_{\mathrm{R}}^{\mathrm{H}} \mathbf{H}_{\mathrm{SR}} \mathbf{\Phi}_{\mathrm{S}}, \quad (15)$$

where $\mathbf{\Phi}_{\mathrm{S}}$ and $\mathbf{\Phi}_{\mathrm{R}}$ are defined as in (7). All relays then transmit orthogonal training sequences to all destinations. Assuming absence of noise, destination m can estimate

$$\widehat{h}_{\mathrm{R}_l\mathrm{D}_m} = h_{\mathrm{R}_l\mathrm{D}_m} e^{j\left(\varphi_{\mathrm{R}_l} + \psi_{\mathrm{R}_l} - \varphi_{\mathrm{D}_m}\right)}, \ \forall\, l = \{1, \dots, N_{\mathrm{R}}\}. \quad (16)$$

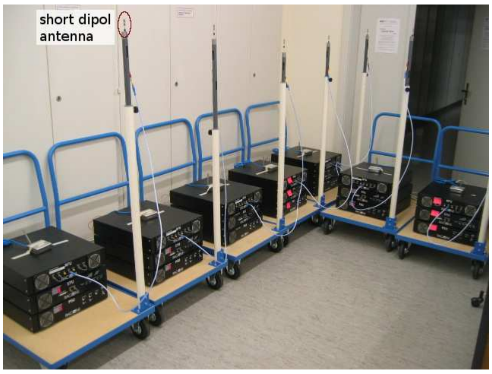

Fig. 2. 7 RACooN nodes placed on carts for mobility. The antennas are mounted at a height of about 1.5 m.

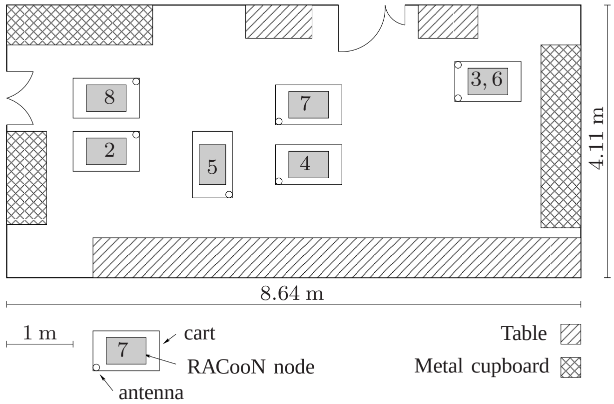

Fig. 3. Measurement setup and topology. The numbers 3–8 indicate the numbering of the RACooN nodes. RACooNs 3 and 6 are stacked on top of each other on the same cart.

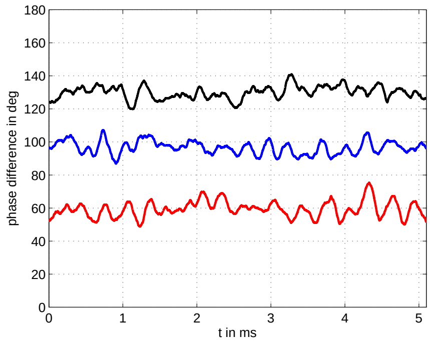

Fig. 4. LO phase difference between 2 RACooN nodes for 3 different measurements.

This requires a total of N_{R} orthogonal sequences. The matrix of estimated second-hop channel coefficients is then

$$\widehat{\mathbf{H}}_{\mathrm{RD}} = \mathbf{\Phi}_{\mathrm{D}}^{\mathrm{H}} \mathbf{H}_{\mathrm{RD}} \mathbf{\Psi}_{\mathrm{R}} \mathbf{\Phi}_{\mathrm{R}}, \quad (17)$$

where the matrix $\mathbf{\Psi}_{\mathrm{R}}$ is defined as in (8). It comprises the changes of the relays' LO phases during the time between reception of the sources' training sequences and transmission of the relay's training sequences. Recall that the nonzero entries of $\mathbf{\Psi}_{\mathrm{R}}$ are random variables.

The required channel estimates finally have to be disseminated to the relays if they are to calculate the gain matrix $\mathbf{G}$ locally.

V. The Demonstrator

We have seen in section III that the received signal $\mathbf{d}$ at the destinations becomes independent of the relays' LO phase offsets when phase noise becomes neglegible and thus $\mathbf{\Psi}_{\mathrm{R}} = \mathbf{I}_{N_{\mathrm{R}}}$. The time between reception and retransmission at the relays has to be short in order to fulfill this. It can easily be verified that in this case also the calculation of the gain matrix becomes independent of $\mathbf{\Phi}_{\mathrm{R}}$ for many gain allocation schemes (e.g. multiuser MMSE relaying [11], multiuser zero-forcing relaying [12], and distributed maximum ratio combining [4]). Other schemes still have to be investigated regarding this issue. This essentially means that we can perform distributed beamforming without requiring a global carrier phase synchronization at the relays. Our demonstrator shows that this works under real-world conditions.

A. The RACooN Lab

RACooN stands for *Radio Access with Cooperating Nodes* and is a custom-built radio testbed at our institute. It comprises 10 identical single-antenna nodes that can transmit and receive at a carrier frequency of 5.1 GHz to 5.9 GHz in a half-duplex manner. Each terminal employs a power supply unit (PU; power supply), a storage unit (STU; baseband processing and data storage), and a RF unit (RFU; radio frequency (RF) part including 16 bit AD/DA converters) (see **Fig. 2**). Individual Rubidium normals are used to provide the clock for each unit. As a consequence each local oscillator exhibits an individual and unknown phase offset that changes due to phase noise. The baseband clock rate is 80 MHz leading to a symbol duration of 12.5 ns. The nodes exhibit user bandwidth with equalized phase response of 60 MHz. Timeslot synchronization takes place using USB cables prior to operation. Each RACooN unit is able to scale and rotate the complex baseband transmit data in realtime. We use this feature to apply a previously calculated, complex gain factor in an amplify-and-forward manner to the transmit data of the nodes that act as relays.

Each RACooN node is placed on a cart to provide mobility. We used self-made short dipole antennas that have been designed for the required frequency range and are mounted on poles at a height of about 1.5m. The measurement environment was a laboratory room in the basement of the university building (see **Fig. 3**). The walls consist of concrete and a row of windows is located in the 'lower' wall. Electronic equipment is placed on the tables. During the measurements no one was in the room to guarantee a static propagation environment.

B. Phase Noise

The received signal at the destinations is a function of the matrix $\mathbf{\Psi}$ (see (10)). It represents the LO phase changes due to phase noise during the processing time at the relay. The LOs of all RACooN nodes certainly exhibit phase noise. In order to assess its severity we monitor the changes between two nodes' LOs using a training sequence of length 5.12 ms (corresponding to 2^{12} samples of length 12.5 ns each). We connect the antenna input/output of the two units via cable to provide a static propagation channel. Then we transmit the training sequence from one unit to the other. At the receiving unit we calculate the phase difference between transmitted and received samples. **Fig. 4** shows the results of three independent measurements that were executed a couple of seconds apart from each other. It can be seen that the LO phase difference varies around a mean value that is approximately constant for each of the observations (roughly $130°$, $95°$, and $55°$, respectively). The mean values themselves have been observed to be independent from each other when the time between consecutive measurements is large (in the order of seconds).

C. Transmission Cycle

Each transmission cycle of the demonstrator comprises 2 phases: in the *training phase* the first and second hop channels are estimated. Based on these estimates, the gain matrix is calculated in a way that it suppresses interuser interference at the destination nodes [12]. Afterwards, in the *evaluation phase*, we estimate the equivalent two-hop channel matrix $\mathbf{H}_{\mathrm{SRD}}$ for the case that the previously calculated gain matrix is used at the relays. As a measure of how good the scheme performed, we finally calculate the SIR at each destination. In the following the two phases are described in detail:

Phase 1 (training phase):

1) All source nodes transmit mutually orthogonal training sequences to all relay nodes. Afterwards, all relay nodes transmit mutually orthogonal training sequences to all destination nodes. We use cyclically shifted m-sequences with a length of 511 samples as training sequences.
2) Knowing the transmitted training sequences, relays and destinations estimate the first-hop and second-hop channels, respectively. The bandwidth of the estimated channels is $80\,\mathrm{MHz}$ since the baseband symbol duration is $12.5\,\mathrm{ns}$. Channel measurements in a similar environment have shown that the 0.9 correlation coherence bandwidth is about 1.6 MHz. We expect to encounter a highly frequency-selective behavior of the channel over the whole $80\,\mathrm{MHz}$ bandwidth. Since we are constrained to a scalar gain factor for each relay we can only work with frequency-flat channels. Therefore we base the calculation of the gain matrix on the channel matrices corresponding to a single frequency bin that is assumed to be frequency flat. We choose the length of the m-sequences used for channel estimation to be equal to 511. The resulting frequency bin size is then $\frac{80\,\mathrm{MHz}}{511} \approx 0.16\,\mathrm{MHz}$, which is roughly 10 percent of the 0.9 correlation coherence bandwidth.
3) A central processor uses the estimated first and second hop channel coefficients to calculate the gain matrix and disseminates the complex gain factors to the respective relay nodes. We use the multiuser zero-forcing (MUZF) gain allocation scheme as in [12] to compute $\mathbf{G}$. It is calculated such that in a perfect world, i.e. $\mathbf{\Psi}_{\mathrm{R}} = \mathbf{I}_{N_{\mathrm{R}}}$, $\widehat{\mathbf{H}}_{\mathrm{SR}} = \mathbf{H}_{\mathrm{SR}}$, and $\widehat{\mathbf{H}}_{\mathrm{RD}} = \mathbf{H}_{\mathrm{RD}}$, all interuser interference is cancelled. The equivalent channel matrix $\mathbf{H}_{\mathrm{SRD}}$ is then diagonal. The relay transmit powers are adjusted by scaling $\mathbf{G}$ such that its squared Frobenius norm is $\|\mathbf{G}\|_{\mathrm{F}}^2 = N_{\mathrm{R}}$.

Phase 2 (evaluation phase):

1) The source nodes transmit mutually orthogonal training sequences to all relay nodes.
2) At the relay nodes we have access to the complex baseband samples of the received signal. Prior to retransmission each relay applies its previously calculated complex gain factor to the samples. Due to constraints imposed by the RACooN hardware, the time between reception and retransmission is at least $1.2\mathrm{ms}$. During that time the LO phases will have changed within a certain range because of phase noise (see **Fig. 4**), i.e. $\mathbf{\Psi}_{\mathrm{R}} \neq \mathbf{I}_{N_{\mathrm{R}}}$ in (10). As a consequence the previously calculated gain matrix no longer diagonalizes the equivalent channel matrix. We expect to observe some interuser interference at the destination nodes due to nonzero offdiagonal elements of $\mathbf{H}_{\mathrm{SRD}}$.
3) Correlating the complex baseband samples of the destinations' received signals with the training sequences, the equivalent two-hop channel matrix $\mathbf{H}_{\mathrm{SRD}}$ is finally computed. The SIR at destination node $m \in \{1, \ldots, N_{\mathrm{D}}\}$ is then defined as

$$\mathrm{SIR}_m = \frac{|\mathbf{H}_{\mathrm{SRD}}[m,m]|^2}{\sum_{\substack{k=1\\k\neq m}}^{N_{\mathrm{S}}} |\mathbf{H}_{\mathrm{SRD}}[m,k]|^2} \tag{18}$$

where we assumed equal transmit power of all sources.

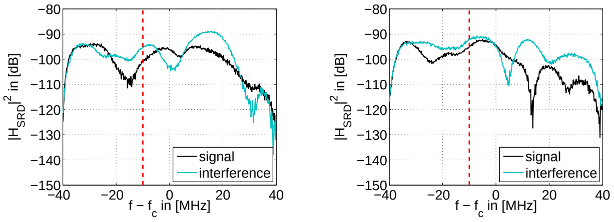

(a) RACooN 6 (b) RACooN 8

Fig. 5. Equivalent two-hop channels for noncoherent forwarding.

VI. Results

For our demonstration we built a system with $N_{\mathrm{S}} = N_{\mathrm{D}} = 2$ source/destination pairs and $N_{\mathrm{R}} = 3$ relays. The topology is as depicted in **Fig. 3**. We define the following source/destination pairs:

- Source 1: RACooN 2, destination 1: RACooN 6
- Source 2: RACooN 3, destination 2: RACooN 8

RACooN nodes 4, 5, and 7 act as relays. **Figs. 5(a)** and **5(b)** show a single realization of the equivalent two-hop channels observed at destination nodes 6 and 8, respectively, for the case that $\mathbf{G} = \mathbf{I}_{N_{\mathrm{R}}}$. We plot the squared magnitude of the equivalent two-hop channel coefficients. The bandwidth of the channel is $80\mathrm{MHz}$ around the carrier frequency $f_{\mathrm{c}} = 5.5\mathrm{GHz}$. Both 10 MHz bands at the border of the 80 MHz band, i.e. from $f_{\mathrm{c}} - 40$ MHz to $f_{\mathrm{c}} - 30$ MHz and from $f_{\mathrm{c}} + 30$ MHz to $f_{\mathrm{c}} + 40$ MHz are strongly influenced by the RACooN frequency response. The curves labeled as 'signal' are related to the channels from the belonging sources whereas the curves labeled as 'interference' are related to the channels from the nonbelonging, i.e. interfering, sources. We call this case *noncoherent forwarding* as the relay gain factors are chosen independently from the channel coefficients. At a frequency of $f - f_{\mathrm{c}} = -10$ MHz, indicated by the dashed vertical line in the plots, the SIR is $-5.0\,\mathrm{dB}$ and $-3.0\,\mathrm{dB}$ at RACooN 6 and RACooN 8, respectively.

In **Figs. 6(a)** and **6(b)** we plot a single realization of the equivalent two hop channels for the case that the gain matrix is chosen according to multiuser zero-forcing relaying. Since the RACooN hardware restricts the AF gains to be scalar (see section V-A), the interference suppression is restricted to a single (frequency-flat) channel bin. We chose $f_{\mathrm{ZF}} = f_{\mathrm{c}} - 10\mathrm{MHz}$ and calculated the gain factors based on the estimated channel coefficients at this frequency. The propagation environment is the same as for Fig. 5. In a perfect world all interuser interference would be cancelled at f_{ZF}. Indeed we observe a reduction of the interference power at both destinations.

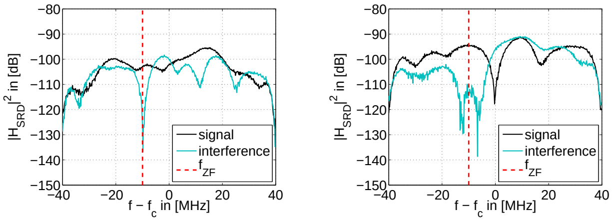

(a) RACooN 6 (b) RACooN 8

Fig. 6. Equivalent two-hop channels for MUZF.

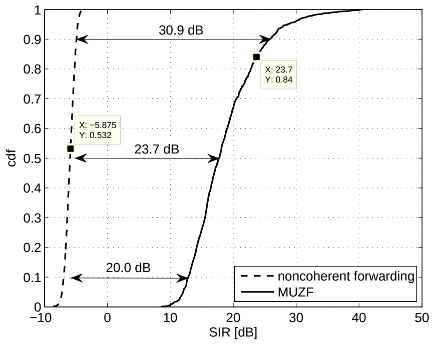

Fig. 7. cdf of the SIR at RACooN node 6 for noncoherent forwarding and MUZF.

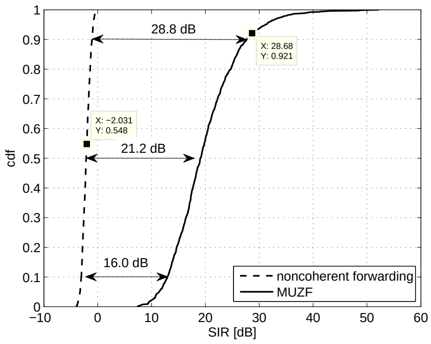

Fig. 8. cdf of the SIR at RACooN node 8 for noncoherent forwarding and MUZF.

At RACooN 6 the gain allocation places a deep notch at approximately f_{ZF} resulting in an SIR of $23.9\,\mathrm{dB}$ (Fig. 6(a)). This is a gain of $28.9\,\mathrm{dB}$ compared to Fig. 5(a). For RACooN 8 the SIR increases from $-3.0\,\mathrm{dB}$ in Fig. 5(b) to $18.65\,\mathrm{dB}$ in Fig. 6(b). However, two deeper notches are placed near but not exactly at f_{ZF}. The reason for this observation is that due to LO phase noise at the relays ($\mathbf{\Psi}_{\mathrm{R}} \neq \mathbf{I}_{N_{\mathrm{R}}}$), the gain allocation does not completely suppress the interference at f_{ZF}. As the channel bins are correlated across frequency, interference is instead suppressed more efficiently at a frequency bin in the vicinity of f_{ZF}. This can then be observed as a shift of the notch in frequency. The two notches in Fig. 6(b) indicate that the frequency bins around $f_{\mathrm{c}} - 13\,\mathrm{MHz}$ and $f_{\mathrm{c}} - 9\,\mathrm{MHz}$ are highly correlated.

In order to get some statistically relevant data we performed 1000 measurements in a static propagation environment for $f_{\mathrm{ZF}} = f_{\mathrm{c}} - 10\,\mathrm{MHz}$. For each realization we calculate the SIR for the noncoherent case as well as the multiuser zero-forcing gain allocation. The cumulative density functions (cdf) of the SIRs are depicted in **Figs. 7** and **8**. We indicate the outage SIR improvements at 0.1, 0.5, and 0.9 outage probabilities. The numbers in the boxes show the respective mean values of all realizations. At RACooN 8 (**Fig. 8**) we gain $16\,\mathrm{dB}$ SIR in 90% of the cases and at RACooN 6 (**Fig. 7**) we even gain $20\,\mathrm{dB}$ SIR in 90% of the cases. This is a motivating result as we face a phase uncertainty in the range of $\pm 10^{\circ}$ at each relay node (see section V-B). A system designed for a shorter processing time could easily perform even better.

VII. Conclusion and Future Work

We presented a demonstrator for linear AF using our RACooN Lab. Building a network with 2 source/destination pairs and 3 relays, the results verify that a global phase reference is not required at the relays for multiuser zero-forcing relaying. Phase noise, however, still has an impact on performance. If the relays' LO phases change during the time between reception and retransmission, performance degrades. Consequently, the shorter the transmission cycle, the more accurate the interference suppression will be. Measurement results showed that our demonstrator is able to suppress inter-user interference at both destinations reasonably well.

Future work will comprise the extension of multiuser zero-forcing relaying to broadband interference suppression using FIR filters at the relays.

References

[1] J. N. Laneman and G. W. Wornell, "Distributed Space-Time-Coded Protocols for Exploiting Cooperative Diversity in Wireless Networks," *IEEE Transactions on Information Theory*, vol. 49, no. 10, pp. 2415–2425, Oct. 2003.

[2] A. Sendonaris, E. Erkip, and B. Aazhang, "User Cooperation Diversity - Part I and II," *IEEE Transactions on Communications*, Nov. 2003.

[3] H. Bölcskei, R. U. Nabar, Ö. Oyman, and A. J. Paulraj, "Capacity scaling laws in MIMO relay networks," *IEEE Transactions on Wireless Communications*, vol. 5, no. 6, Jun. 2006.

[4] Y.-S. Tu and G. J. Pottie, "Coherent cooperative transmission from multiple adjacent antennas to a distant stationary antenna through AWGN channels," in *Proc. IEEE VTC'02 Spring, Birmingham, Al*, vol. 1, 2002, pp. 130 – 134.

[5] G. Barriac, R. Mudumbai, and U. Madhow, "Distributed beamforming for information transfer in sensor networks," in *IPSN'04: Proc. of the Third International Symposium on Information Processing in Sensor Networks*, 2004, pp. 81 – 88.

[6] S. Berger and A. Wittneben, "Carrier phase synchronization of multiple distributed nodes in a wireless network," IEEE Workshop on Signal Processing Advances in Wireless Communications (SPAWC), Helsinki, Jun. 2007.

[7] ——, "Coherent multiuser relaying without global phase reference: A zero-forcing approach," *IEEE Transactions on Wireless Communications*, submitted.

[8] A. Demir, A. Mehrotra, and J. Roychowdhry, "Phase noise in oscillators: A unifying theory and numerical methods for characterization," *IEEE Transactions on Ciruits and Systems – I: Fundamental Theory and Applications*, vol. 47, no. 5, pp. 655 – 674, May 2000.

[9] A. Wittneben and B. Rankov, "Distributed Antenna Systems and Linear Relaying for Gigabit MIMO Wireless," in *Proc. IEEE VTC'04 Fall, Los Angeles*, Sep. 2004.

[10] L. Tomba, "On the effect of wiener phase noise in OFDM systems," *IEEE Transactions on Communications*, vol. 46, no. 5, pp. 580–583, May 1998.

[11] S. Berger and A. Wittneben, "Cooperative Distributed Multiuser MMSE Relaying in Wireless Ad-Hoc Networks," in *Asilomar Conference on Signals, Systems, and Computers, Pacific Grove, CA*, Oct./Nov. 2005.

[12] A. Wittneben, "Coherent Multiuser Relaying with Partial Relay Cooperation," *IEEE Wireless Communication and Networking Conference (WCNC), Las Vegas, NV, USA*, Apr. 2006.